Published in final edited form as:

Magn Reson Imaging Clin N Am. 2016 February ; 24(1): 223–238. doi:10.1016/j.mric.2015.08.012.

Multiparametric Breast MRI of Breast Cancer

Habib Rahbar, MD and **Savannah C. Partridge, PhD**

University of Washington, Seattle Cancer Care Alliance, Department of Radiology, Breast Imaging Section, 825 Eastlake Avenue East, P.O. Box 19023, Seattle, WA 98109–1023, USA

Synopsis

Breast MRI has increased in popularity over the past two decades due to evidence for its high sensitivity for cancer detection. Current clinical MRI approaches rely on the use of a dynamic contrast enhanced (DCE-MRI) acquisition that facilitates morphologic and semi-quantitative kinetic assessments of breast lesions. The use of more functional and quantitative parameters, such as pharmacokinetic features from high temporal resolution DCE-MRI, apparent diffusion coefficient (ADC) and intravoxel incoherent motion (IVIM) on diffusion weighted MRI, and choline concentrations on MR spectroscopy, hold promise to broaden the utility of MRI and improve its specificity. However, due to wide variations in approach among centers for measuring these parameters and the considerable technical challenges, robust multicenter data supporting their routine use is not yet available, limiting current applications of many of these tools to research purposes.

Keywords

Multiparametric breast MRI; dynamic contrast enhanced; diffusion weighted imaging; magnetic resonance spectroscopy; breast cancer

Introduction

Breast cancer is extremely common, striking one in eight American women, and is the second leading cause of cancer death among women in the United States (1). Breast cancer mortality has decreased substantially over the past several decades, owing both to earlier stage breast cancer detection through improved imaging techniques and improved therapeutics. Although breast MRI is a relatively recent imaging technique, it was first proposed to aid early breast cancer detection in the 1970s (2), which was supported by the discovery that abnormal breast tissue demonstrates differences in longitudinal (T1) and transverse (T2) relaxation times in vitro when compared to normal tissue (3). However, it was not until the elucidation that most breast cancers demonstrate higher signal on T1 weighted images after the administration of gadolinium-based contrast material that breast

Corresponding Author: Savannah C. Partridge, PhD (Address as above), scp3@uw.edu, Phone: 206-288-1306, Fax: 206-288-6573.

MRI became a widely used tool for in vivo characterization of breast cancer (4). Although optimal evidence-based uses continue to evolve, common clinical indications for conventional contrast-enhanced breast MRI currently include supplemental screening for high-risk women, pre-operative evaluation of breast cancer extent of disease, assessment of equivocal findings on standard imaging and/or clinical exam, and evaluation of breast cancer response to neoadjuvant chemotherapy.

Perhaps the greatest driving force behind the increasingly wide adoption of breast MRI at many centers is its exquisite sensitivity (reported to approach 100%) for breast cancer detection. Multiple studies have shown that conventional contrast-enhanced breast MRI has the highest sensitivity of any imaging modality for breast cancer detection in asymptomatic high-risk women (5–8) and mammographically and clinically occult additional disease in the contralateral (6) and ipsilateral breast (9) in patients with recently diagnosed breast cancer. However, a major barrier to wider adoption of this technique for average and intermediate risk patients is its modest specificity due to overlap in the imaging features of benign and malignant lesions, with wide variations in the positive predictive value (PPV) of breast MRI reported in the literature (24 to 89%) (10).

MRI also has been increasingly been studied as a tool to determine which newly diagnosed breast cancers are likely to respond to pre-surgical, or neoadjuvant, chemotherapy. Several early studies examining the use of MRI to assess early response to neoadjuvant chemotherapy found that changes in size or volume and enhancement kinetic profiles on MRI were associated with favorable responses to therapy, including pathologic complete response (pCR) (11, 12). These findings suggested that MRI could be used to optimize medical therapy regimens for each individual. The general superiority of MRI over clinical examination and standard imaging techniques for predicting pCR was suggested in multiple single center studies (13, 14), and confirmed in a large multi-center trial (15). Though standard contrast-enhanced MRI is the most accurate modality for predicting important neoadjuvant therapy outcomes, its clinical impact has been limited by its cost and modest overall performance in this setting.

Although MRI is commonly used at many centers to further evaluate equivocally suspicious clinical or imaging findings, several obstacles have limited application of MRI in this clinical setting. Barriers to cost-effective implementation of MRI to reduce unnecessary biopsies prompted by conventional imaging or clinical exam include the relatively low cost associated with image-guided biopsies, which are highly accurate and safe, compared with serial imaging (16) and the high negative predictive value (NPV) (~98%) needed to obviate the biopsy of a suspicious finding based on current American College of Radiology (ACR) Breast Imaging Reporting and Data System (BI-RADS) guidelines (17). Early studies have demonstrated that the NPV of MRI for this clinical indication ranges from 76% for further evaluation of suspicious mammographic calcifications (18) to 85% in the setting of any suspicious mammographic or clinical finding (19). Studies from our institution found that while breast MRI has high sensitivity and high NPV for this clinical indication, the added breast cancer yield was too low to routinely recommend breast MRI for problem solving (20). More recently, Strobel et al found that suspicious (BI-RADS category 4) findings identified on screening mammography or ultrasound that were further evaluated using

conventional breast MRI could help avoid up to 92% of unnecessary biopsies, and was particularly accurate for sonographic findings and mammographic findings that did not include lesions comprised entirely of calcifications (21).

The basis for the strong clinical performance of conventional breast MRI has been through utilization of an imaging approach that emphasizes anatomic and morphologic detail through high spatial resolution and limited temporal resolution dynamic contrast enhanced (DCE-MRI) technique. This approach provides limited insight on physiologic features of breast tissue and pathology through the measurement of semi-quantitative kinetic features. While these basic kinetic enhancement features, including peak initial phase and delayed phase curve descriptors, have shown some ability to distinguish between malignant and benign lesions (22), they in general have provided a small incremental value to standard morphological descriptions (19). As a result, there is increasing interest in exploring whether multiparametric approaches to breast MRI that incorporate more highly quantitative pharmacokinetic DCE-MRI modeling and other functional MRI techniques, such as diffusion weighted imaging (DWI) and magnetic resonance spectroscopy (MRS), to probe specific biological properties such as abnormal vessel permeability, cellularity, and chemical composition, can further advance the use of MRI for these specific clinical settings.

Breast MRI Parameters

There is no single way to achieve high quality breast MRI, and this is particularly true when considering a multiparametric approach to MRI acquisition. Nonetheless, MRI should include an acquisition utilizing a high field (B_0) magnet (≥1.5T) that is bilateral with complete breast and axilla coverage. Only dedicated breast surface coils are appropriate for breast MRI applications, as the built-in body coil cannot provide enough signal-to-noise (SNR) for high quality breast imaging.

Dynamic Contrast Enhanced (DCE) MRI

Currently, a DCE-MRI acquisition is central to breast MRI protocols, and the ACR Breast MRI Accreditation Program (BMRAP) mandates that a multiphase T1-weighted acquisition be performed for clinical breast MRI. Due to time and technical restraints, DCE-MRI protocols generally emphasize either high spatial resolution and full coverage or high temporal resolution in imaging of contrast uptake kinetics in breast. However, more sophisticated acquisition strategies that “under-sample” the periphery of k space on subsequent dynamic acquisitions and more frequently sample the center of k space can provide simultaneous high spatial, high temporal resolution acquisitions with full bilateral coverage (23–25), (Fig. 1). There is wide variation among centers on the number of post-contrast phases acquired. The ACR BMRAP requires acquisition of a minimum of two post contrast T1 weighted images, with the first post-contrast sequence acquired within 4 minutes of contrast injection. DCE-MRI acquisition provides two primary imaging features that can be used to evaluate breast lesions: morphology and kinetic enhancement characteristics.

Morphology—There are three general morphologic descriptors of enhancing findings of the breast, which are defined by the ACR BI-RADS atlas: foci, masses, and non-mass enhancement (NME). Masses and NMEs also have additional descriptors that can further

refine an interpreting radiologist's suspicion for malignancy. Prior studies have shown that morphologic features are perhaps the most important factor for initial assessment of likelihood of malignancy of a given lesion (19). Suspicious morphologic features for masses include irregular shape, heterogeneous or rim internal enhancement, and irregular or spiculated margins. Suspicious NME morphologic features include segmental or linear distribution with heterogeneous or clustered ring enhancement. Breast cancers that present as NME are more likely to reflect in situ carcinoma than masses; however, significant overlap exists in morphologic presentation on MRI of invasive breast cancer, ductal carcinoma in situ, and atypical/high-risk lesions.

DCE kinetic enhancement features—Differential enhancement of malignancies relative to normal breast tissue is based on the fact that malignancies typically recruit abnormal new blood vessels to support their growth (i.e. angiogenesis). The rate at which these abnormal vessels allow nutrients to spill into a tumor and the rate cell cycle byproducts are removed from a tumor can be characterized through assessing kinetic enhancement curves obtained from DCE-MRI. Most commonly, breast kinetic enhancement features are measured semi-quantitatively using modest temporal resolution with at least two to three post-contrast T1-weighted acquisitions, with k-space centered at approximately 90 to 120 seconds after contrast injection for the first post-contrast images. Using the data obtained at each of these time points, a time-signal intensity curve can be determined for a given lesion or region of interest (ROI), allowing assessment of two phases of enhancement: initial phase, within approximately two minutes of contrast injection, and late (or delayed) phase, after two minutes or after peak enhancement (Fig. 2). In the initial phase, enhancement classifications of "slow", "medium", and "fast" are determined by signal intensity increase defined by the equation:

$$\mathrm{SI}_{\%\mathrm{increase}}=[(\mathrm{SI}_{\mathrm{post}}-\mathrm{SI}_{\mathrm{pre}})/\mathrm{SI}_{\mathrm{pre}}]\times 100\%$$

where SI_{pre} is the baseline signal intensity of a region of interest and SI_{post} is the signal intensity of the same region of interest after contrast injection. In the delayed phase, enhancement curves can be classified by three basic curve types: persistent, plateau, and washout. Persistent delayed enhancement is generally considered to be a benign enhancement curve type, while plateau delayed enhancement is of intermediate suspicion for malignancy and washout delayed enhancement is the most suggestive of malignancy. Although the most classic combined curve type for malignant breast lesions is fast initial enhancement followed by early washout (sometimes referred to as a type III curve (26)), there is significant overlap of semi-quantitative kinetic curve types among benign and malignant lesions.

MRI techniques that acquire post contrast images with high temporal resolution can allow for more elegant assessment of contrast kinetics through pharmacokinetic modeling techniques. Pharmacokinetic models enable quantitative assessments of contrast agent exchange between the intravascular and the interstitial space, providing measures related to tumor blood flow, microvasculature, and capillary permeability. A two-compartment model is the most commonly used approach, measuring the exchange of contrast between tissue (in

this case breast tissue) and the plasma space, and was first proposed in an MRI-context by Tofts and Kermode (27). The concentrations of the gadolinium tracer for each compartment vary with time after the bolus injection of the contrast agent, and quantitative metrics can be measured by this model using the following relationship

$$k_{ep} = K^{trans} / v_e$$

where the volume transfer constant K^{trans} reflects the rate of transfer of gadolinium from plasma to the tissue (units: min^{-1}), (Fig. 1D), the transfer rate constant k_{ep} (min^{-1}) reflects the reflux of contrast agent from the extravascular extracellular space to the plasma compartment, and v_e (%) reflects the leakage of fractional volume from the extravascular extracellular space into the plasma compartment.

Promising clinical applications of quantitative DCE MRI—Multiple authors have demonstrated that some of these pharmacokinetic parameters, particularly K^{trans} and k_{ep}, hold value for improved discrimination of malignant from benign breast pathologies, and may even be used as biomarkers of disease subtypes. Li and colleagues demonstrated that K^{trans} and k_{ep} values progressively increased when measuring normal glands, benign lesions, and malignant lesions, respectively, noting that invasive ductal carcinomas and ductal carcinoma in situ lesions exhibited significantly higher K^{trans} and k_{ep} values than ductal dysplasias (28). Huang et al demonstrated that using K^{trans} values of lesions found to be suspicious on standard clinical breast MRI, a potential “cutoff” value could be used such that lesions with lower K^{trans} values could avoid biopsy and thereby decrease false positive MR examinations (29). Finally, DCE-MRI holds potential for assessing alterations in tumor perfusion in response to preoperative therapies (Fig 3). K^{trans} values have been shown in a recent meta-analysis to be among the most promising MRI parameters for prediction of near pathologic complete response to neoadjuvant chemotherapy, outperforming standard tumor size measurements (30).

Technical challenges and considerations of quantitative DCE-MRI—In order to perform DCE-MRI pharmacokinetic modeling and calculate quantitative parameters, knowledge of both the pre-contrast T1 relaxation times of the tumor or tissue being imaged and the arterial input function (AIF), or the concentration of contrast agent as it changes over time within the arterial blood, is required. Measuring each of these parameters introduces unique challenges and potential for error. Pre-contrast T1 mapping is an essential step to convert DCE-MRI signal intensity into contrast agent concentration. T1 mapping requires acquisition of an additional series of images prior to DCE MRI, most commonly using varying flip angle or inversion recovery approaches, and thus adds to the overall examination times. Moreover, variable flip angle approaches are prone to inaccuracies due to B1 inhomogeneity, a common issue for breast imaging, particularly at higher field strengths (31). Most models require that the AIF be measured directly for each subject (32), which is often challenging to perform and necessitates acquisition tradeoffs (in coverage and/or spatial resolution) to achieve the very high temporal resolution required to accurately sample the rapidly changing AIF. Furthermore, AIF measures can be very sensitive to

patient motion between dynamic acquisitions. One common approach to avoid the challenge of directly calculating the AIF is to employ an average AIF calculated from a larger population for whom the injection site, dose, and rate were kept constant (29). Yankeelov et al have proposed another method to circumvent this problem by estimating the AIF using a reference region model, and found that such an approach correlated well with direct AIF measurement (33). Novel high spatiotemporal DCE-MRI acquisition strategies, as described earlier, hold potential to provide high temporal resolution sampling of contrast enhancement curves without undesirable tradeoffs in spatial resolution and coverage, which may improve feasibility for utilization of pharmacokinetic analysis in clinical breast applications (25).

Theoretically, model-based pharmacokinetic parameters have the advantage over semi-quantitative enhancement curve assessments of being objective measures of underlying physiology that are not affected by variability in scan parameters. However, given the different modeling algorithms, multiple challenges and varying potential solutions, each of which can create significant differences in quantitative measurements, the generalizability of individual studies of advanced pharmacokinetic parameters will require standardization of the technical approach and multicenter testing (34).

Diffusion Weighted MRI (DWI)

DWI is a non-contrast MRI technique that measures the mobility of water molecules in vivo and probes tissue organization at the microscopic level. This water movement due to molecular diffusion, called Brownian motion, is random in pure water. However, the motion of water molecules in vivo is restricted by hindrances within intracellular and extracellular compartments. As a result, DWI reflects the microscopic cellular environment and is sensitive to biophysical characteristics such as cell density, membrane integrity, and microstructure.

DWI has shown promise for the detection and characterization of breast cancer (35). Numerous studies have shown that malignant breast lesions exhibit decreased water diffusion, attributed primarily to the increased cell density associated with breast tumors (36). DWI is a short scan available on most commercial MR scanners that does not require any exogenous contrast and can be added to breast MR imaging examinations to provide additional unique information on tissue microstructural properties.

Apparent diffusion coefficient (ADC) calculation—DWI utilizes motion-sensitizing gradients during MR image acquisition to probe local diffusion characteristics. The diffusion-weighted MRI signal is reduced in intensity proportional to the water mobility, and is commonly described by the monoexponential equation:

$$S_D = S_0 e^{-b*ADC} \quad (2)$$

where S_0 is the signal intensity without diffusion weighting, S_D is the signal intensity with diffusion weighting, b is the applied diffusion sensitization (s/mm^2), and ADC is the apparent diffusion coefficient, defined as the average area a water molecule occupies per unit time (mm^2/s) (37). In general, ADC can be calculated directly from a minimum of two acquisitions with different b-values using:

$$ADC = \ln(S_1/S_2)/(b_2 - b_1) \quad (3)$$

where b_1 is the minimum b-value (eg, 0 s/mm^2) and b_2 is the maximum b-value (e.g. 800 s/mm^2), S_1 is the signal intensity at b = b_1, S_2 is the signal intensity at b = b_2, and repetition time (TR) and echo time (TE) remain constant (38). Due to restricted diffusion, breast malignancies commonly exhibit hyperintensity on DWI and lower ADC relative to normal breast parenchyma (Fig 4).

Promising clinical applications of breast DWI—DWI holds strong potential as an adjunct MRI technique to reduce false positives and unnecessary biopsies. This has been the most widely explored application of DWI for breast imaging, and numerous groups have demonstrated restricted water diffusion in breast malignancies and significant differences in ADC values of benign and malignant lesions (36, 39–41) (Figs. 5, 6 and 7). A meta-analysis of 13 studies evaluating the diagnostic performance of DWI in 964 breast lesions (615 malignant, 349 benign) reported a pooled sensitivity of 84% (95% confidence interval [CI]: 82%, 87%) and specificity of 79% (95% CI: 75%, 82%). ADC values for malignancies ranged from 0.87 to 1.36 $\times 10^{-3}$ mm^2/s, and recommended threshold ADC cutoffs to discriminate benign and malignant lesions varied from 0.90 to 1.76 $\times 10^{-3}$ mm^2/s (with 10/13 studies using a maximum b value of 1000 s/mm^2) (42). Further, multiple studies across a variety of field strengths have found that ADC measures are complementary to DCE-MRI parameters for discriminating benign and malignant breast lesions and can increase the accuracy of conventional breast MRI assessment (43–46).

Another promising application for DWI is in monitoring of breast cancer treatment. Alterations in cell membrane integrity and reduced tumor cellularity due to cytotoxic effects of chemotherapy result in increased water mobility within the damaged tumor tissue. A corresponding increase in tumor ADC in response to treatment may be detectable earlier than changes in tumor size or vascularity as measured by DCE-MRI, suggesting DWI may provide valuable early indication of treatment efficacy (47, 48). In a recent study of 118 women undergoing neoadjuvant chemotherapy for locally advanced breast cancer, Richard et al found that pretreatment tumor ADC values differed between intrinsic subtypes and were predictive of pathological response in triple-negative tumors (49).

DWI may also offer a viable non-contrast method of breast MR screening. Many mammographically and clinically occult breast cancers detected by DCE-MRI are also visible on DWI, and can be differentiated from benign breast lesions based on ADC (50). In one study of asymptomatic women, DWI provided higher accuracy than screening mammography for the detection of breast malignancies (51). The potential of DWI as a non-contrast alternative for breast MR screening has only been explored in a handful of studies and requires further investigation.

Technical challenges of breast DWI—Although a growing number of imaging centers are incorporating DWI into the clinical breast MR examination, several factors currently limit widespread clinical implementation (35). The techniques used to acquire DW images of the breast, including the choice of b-values, vary considerably across studies in the

literature. There is also wide variation in image quality of breast DWI due to the particular challenges of off-isocenter imaging, air-tissue interfaces, and significant fat content in the breast. Complete fat suppression is necessary to avoid detrimental chemical shift artifacts in echo planar DWI and confounding effects of residual intravoxel fat signal on breast tissue ADC measures (52). Furthermore, differences in data analysis approaches including post-processing, ADC calculation, and region-of-interest methods result in considerable differences in the reported ADC values of similar breast pathologies. This lack of standardization in image acquisition and post-processing methods makes it difficult to define generalizable interpretation strategies for breast DWI and to reliably assess the clinical utility of the technique.

Advanced methods of breast DWI—A number of compelling advancements in DWI acquisition strategies are under development to overcome the technical issues of spatial distortion and low resolution that currently prevent direct correlation and one-to-one mapping of DCE-MRI and DWI features and limit clinical implementation of breast DWI (53–56). Furthermore, advanced modeling approaches are also being investigated to extract more valuable biological information from breast DWI scans. These include intravoxel incoherent motion (IVIM) modeling, which provides characterization of tissue perfusion in addition to diffusion (57–60); diffusion kurtosis modeling, which characterizes deviation from unrestricted diffusion behavior (evident in vivo at high b-values >1500 s/mm^2) and accounts for ‘tissue complexity’ or physical barriers to diffusion within tissue (cell membranes, organelles, stromal desmoplasia, etc.) (58, 61); and diffusion tensor imaging (DTI), which characterizes the directionality of water diffusion in addition to the rate and may provide further insights on glandular organization (ducts, lobules) and microarchitecture (62–64).

Magnetic Resonance Spectroscopy

Magnetic resonance spectroscopy (MRS) is a noninvasive technique that reflects the chemical composition of tissue. Rather than images, MRS techniques produce spatially-localized signal spectra, with spectral peaks representing the structure and concentration of different chemical compounds in that region. MRS can differentiate tissue states such as normal, malignant, necrotic, or hypoxic based on varying levels of associated detectable metabolites. Proton MRS studies of the breast have demonstrated highly elevated levels of the metabolite choline in malignant lesions compared with benign lesions and normal breast tissue (65–68). The choline peak observed in vivo, located at approximately 3.2 ppm, actually represents a composite of several different choline-containing compounds (including free choline, phosphocoline and glycerophosphocholine, resolvable using ex vivo methods (69)) and is typically referred to as ‘total choline’ (tCho). Choline is known to be involved in cell membrane turnover (phospholipid synthesis and degradation) and is therefore generally considered a marker of cell proliferation. While the underlying biochemical process is not yet well-understood, elevated choline signal in malignancies is thought to result from a combination of both increased intracellular phosphocholine concentration and increased cell density in the lesion (69, 70).

Techniques for acquisition and analysis of breast MRS have been reviewed extensively in a recent article by Bolan (71). In general, single voxel MRS is the most widely used acquisition approach, which produces a single spatially localized spectrum representing the average chemical signal from a 3-dimensional cuboid volume (voxel) centered within a lesion identified on contrast-enhanced MRI (Fig. 8). Some manufacturers currently offer single voxel protocols specifically optimized for breast MRS. An alternative localization technique is chemical-shift imaging (CSI) or MR spectroscopic imaging (MRSI), in which a larger volume is excited and 2D or 3D phase encoding is used to produce a spatially resolved grid of spectra. Breast MRS analysis centers on evaluation of the tCho signal, and has been performed using a variety of approaches that can be generally categorized as (1) qualitative - detection of the presence of a tCho peak, (2) semi-quantitative – measurement of tCho SNR, peak height or peak integral, or (3) absolute quantification – calculation of tCho concentration (using internal referencing to unsuppressed water signal or external referencing to a phantom with a known chemical concentration) (71).

Promising clinical applications of breast MRS—MRS may help to improve the accuracy of diagnosing suspicious breast lesions on MRI. ^{1}H-MRS measures of choline levels in suspicious breast lesions have been shown to provide high specificity for distinguishing benign from malignant lesions (72–74). The majority of breast MRS studies to date have been performed at 1.5T using single voxel approaches. In a recent meta-analysis of 19 breast MRS studies including 1198 lesions (773 malignant, 452 benign), Baltzer and Dietzel found a pooled sensitivity of 73% (95% CI: 85%, 91%) and specificity of 88% (95% CI: 64%, 82%) for lesion diagnosis (75). Their analysis did not show any significant performance advantages of 3T over 1.5T field strength or MRSI over single voxel techniques, or qualitative over quantitative tCho assessments, although the numbers of studies using 3T (n=2/19) and MRSI (n=3/19) were small. More recently, Pinker et al have reported a high diagnostic accuracy for assessing suspicious breast lesions using a multiparametric MRI breast examination incorporating MRSI (76).

Whereas simple qualitative detection of the presence of a tCho peak was a reliable marker of malignancy in earlier investigations (77), newer approaches using higher field strengths and higher sensitivity breast coil designs require more quantitative diagnostic methods because choline also becomes detectable even in normal breast tissue at higher SNR levels (71, 78). A threshold of tCho SNR > 2 is a commonly used threshold for malignancy in prior studies.

Breast MRS may play a valuable role in assessing response to neoadjuvant therapy. Breast tumor choline levels may reflect treatment-induced alterations in cell proliferation prior to any changes in tumor size and thus provide an early predictive marker of treatment response. In support of this, Meisamy and colleagues (70, 79) found acute decreases in tumor tCho concentration were measurable at 4T as early as 24 hours after the first-dose of chemotherapy and correlated with final changes in tumor size. In a large study of 184 patients with breast cancer, Shin et al further showed that tumor tCho measures were higher in invasive versus in situ cancers, and correlated with several prognostic factors including nuclear grade, histologic grade, and estrogen receptor (ER) status (80).

Technical challenges of breast MRS—There are several challenges to routine clinical use of MRS of the breast. As with breast DWI, high quality shimming and lipid suppression are critical for successful breast MRS. Poor shimming results in B0 field inhomogeneities that broaden spectral line widths, causing reduced SNR and a reduced ability to separate different chemical resonances, and may also compromise the performance of chemically selective fat and water suppression in localized MRS. Shimming can be especially challenging in the breast with regions of mixed fibroglandular and adipose tissues and in the presence of metallic biopsy clips. Without adequate fat suppression, lipid sidebands can obscure choline peaks in the spectra. A variety of fat suppression strategies have been used across prior breast MRS studies and there is no clear consensus on the optimal method (71, 75).

A major limitation of breast MRS with current approaches is low sensitivity for detecting choline levels in smaller lesions (<10mm) (71), which limits the applicability of the technique as an adjunct to clinical breast MRI to reduce false positives. Although breast tumor choline levels can be successfully measured using 1.5T MR scanners, increases in both SNR and spectral resolution at higher field strength can improve choline detectability, decrease measurement errors, and enable the assessment of smaller lesions (70). Another factor limiting clinical implementation is that single voxel MRS requires voxel placement to be performed at the time of acquisition, which can be disruptive to clinical workflow as it requires real-time review by experienced radiologists specializing in breast MRI and some level of operator expertise. Furthermore, a single-voxel MRS technique is not helpful for breast cancer screening because of the limitations in breast coverage and voxel localization. Alternatively, multi-voxel MRS approaches are under investigation and hold strong potential for improving the clinical utility of MRS for lesion detection and local staging of disease, as described below.

Advanced methods of breast MRS—Magnetic resonance spectroscopic imaging (MRSI), or chemical shift imaging (CSI), is a multi-voxel approach that enables more extensive spatial sampling of the breast, providing several potential advantages over single-voxel methods. These include the ability to evaluate multiple lesions simultaneously, to characterize tumor heterogeneity, and to assess the extent of disease infiltration into surrounding tissue (81). By providing wider coverage, MRSI reduces the need for a priori knowledge of lesion location and real-time expertise during the MR scan, and may increase the feasibility to perform MRS in screening examinations. Furthermore, MRSI also allows for internal referencing for signal normalization. However, MRSI is more technically challenging than single-voxel MRS with regard to shimming and fat suppression and requires longer scan times to achieve the extended breast coverage, and as a result has not been widely implemented. With advancements in MRI hardware and software, a growing number of groups are implementing breast MRSI research protocols (78, 82–86).

A compelling alternative to conventional ^{1}H MRS, ^{31}P phosphorus MRS holds promise to overcome some of the current challenges of breast MRS. ^{31}P MRS enables direct measurement of phosphocholine and other key metabolites, without the issues of lipid contamination present in ^{1}H MRS signal. Due to the inherently low SNR of ^{31}P MRS caused by low abundance of phosphorus in the body, this approach becomes more feasible at high

field strengths (87). A recent study at 7T demonstrated associations between relative levels of ^{31}P MRS phosphodiester (PDE) and phosphomonoester (PME) peaks and metabolic activity as assessed by mitotic count in breast cancers (88)

Emerging Functional Breast MRI Approaches

There are a number of other functional MRI approaches at early stages of development that are showing promise for advancing breast cancer characterization in preliminary investigations. These include ^{23}Na sodium MRI and blood oxygen level-dependent (BOLD) MRI, described briefly below, as well as other techniques such as MR elastography (89), chemical exchange saturation transfer (CEST) (90, 91), and high spectral spatial resolution (HiSS) imaging (92) that are beyond the scope of this article.

Sodium MRI—While MRI is typically performed to image the hydrogen (^{1}H) nucleus, it can also image other nuclei, such as sodium (^{23}Na). Sodium is present at abundant levels in the body and has important biologic implications. Physiological and biochemical changes associated with proliferating malignant tumors lead to an increase in tissue sodium. Sodium MRI may provide valuable insights to breast tumor metabolism and response to therapy. ^{23}Na sodium MRI studies have demonstrated elevated sodium levels in breast malignancies (93) and have shown that decreases in tumor sodium concentrations may reflect changes in cellular metabolism and membrane integrity with effective treatment (94).

Blood oxygen level-dependent (BOLD) MRI—Blood oxygen level-dependent (BOLD) MRI, also known as intrinsic susceptibility weighted imaging (SWI), can provide a non-invasive method of indirectly measuring tumor perfusion and hypoxia. Tumor hypoxia, a condition of low oxygenation, is a common feature of many solid tumors as rapidly proliferating cells outgrow the existing vasculature. Increased levels of paramagnetic deoxyhemoglobin concentration provide an endogenous contrast agent for imaging tissue hypoxia using BOLD MRI (95, 96). Tumor hypoxia is associated with tumor progression, angiogenesis, treatment resistance, local recurrence, and metastasis (97), and may be a useful biomarker of breast cancer prognosis and response to chemotherapy. BOLD for breast cancer is at an early stage of implementation and optimization, with only a few published studies to date (95, 96, 98, 99).

Conclusion

Perhaps more than any other organ system, the breast holds great potential for clinical benefit from the use of a multiparametric MRI approach. This is due in part to the already broad use of breast MRI in clinical practice, which allows for relatively rapid translation of novel imaging techniques. Several groups have implemented sophisticated multiparametric functional MRI examinations to characterize breast lesions, and have demonstrated dramatic ability to improve the diagnostic accuracy of conventional contrast-enhanced breast MRI (76), to predict and monitor response to medical therapies (94, 100, 101), and to discriminate biological subtypes of cancer (88). However, there are obstacles to routine clinical application of advanced multiparametric breast MRI. Future work to address the many technical challenges unique to each of the individual functional MRI parameters and the lack of standardization of imaging approaches across institutions is needed. Ultimately,

multicenter trials must be conducted (several of which are currently underway through ACRIN (102–104)) to validate single-institution findings prior to widespread implementation of these advanced functional breast MRI techniques.

Acknowledgments

Drs. Rahbar and Partridge have received support from the following grants: National Institutes of Health (NIH): R01CA151326 and P50CA138293 Radiological Society of North America (RSNA): Research Scholar Grant (Rahbar, P.I.).

References

1. American Cancer Society. Breast Cancer Facts and Figures. Atlanta, GA: 2007–2008.
2. Damadian R. Tumor detection by nuclear magnetic resonance. Science. 1971; 171(3976):1151–3. Epub 1971/03/19. [PubMed: 5544870]
3. Bovee WM, Getreuer KW, Smidt J, Lindeman J. Nuclear magnetic resonance and detection of human breast tumor. J Natl Cancer Inst. 1978; 61(1):53–5. Epub 1978/07/01. [PubMed: 276638]
4. Kaiser WA, Zeitler E. MR imaging of the breast: fast imaging sequences with and without Gd-DTPA. Preliminary observations. Radiology. 1989; 170(3 Pt 1):681–6. Epub 1989/03/01. 10.1148/radiology.170.3.2916021 [PubMed: 2916021]
5. Kriege M, Brekelmans CT, Boetes C, Besnard PE, Zonderland HM, Obdeijn IM, et al. Efficacy of MRI and mammography for breast-cancer screening in women with a familial or genetic predisposition. N Engl J Med. 2004; 351(5):427–37. [PubMed: 15282350]
6. Lehman CD, Isaacs C, Schnall MD, Pisano ED, Ascher SM, Weatherall PT, et al. Cancer yield of mammography, MR, and US in high-risk women: prospective multi-institution breast cancer screening study. Radiology. 2007; 244(2):381–8. [PubMed: 17641362]
7. Saslow D, Boetes C, Burke W, Harms S, Leach MO, Lehman CD, et al. American Cancer Society guidelines for breast screening with MRI as an adjunct to mammography. CA Cancer J Clin. 2007; 57(2):75–89. [PubMed: 17392385]
8. Warner E, Plewes DB, Hill KA, Causer PA, Zubovits JT, Jong RA, et al. Surveillance of BRCA1 and BRCA2 mutation carriers with magnetic resonance imaging, ultrasound, mammography, and clinical breast examination. Jama. 2004; 292(11):1317–25. [PubMed: 15367553]
9. Schnall MD, Blume J, Bluemke DA, Deangelis GA, Debruhl N, Harms S, et al. MRI detection of distinct incidental cancer in women with primary breast cancer studied in IBMC 6883. J Surg Oncol. 2005; 92(1):32–8. [PubMed: 16180227]
10. Elmore JG, Armstrong K, Lehman CD, Fletcher SW. Screening for breast cancer. Jama. 2005; 293(10):1245–56. [PubMed: 15755947]
11. Martincich L, Montemurro F, De Rosa G, Marra V, Ponzone R, Cirillo S, et al. Monitoring response to primary chemotherapy in breast cancer using dynamic contrast-enhanced magnetic resonance imaging. Breast Cancer Res Treat. 2004; 83(1):67–76.10.1023/B:BREA.0000010700.11092.f4 [PubMed: 14997056]
12. Pickles MD, Lowry M, Manton DJ, Gibbs P, Turnbull LW. Role of dynamic contrast enhanced MRI in monitoring early response of locally advanced breast cancer to neoadjuvant chemotherapy. Breast Cancer Res Treat. 2005; 91(1):1–10.10.1007/s10549-004-5819-2 [PubMed: 15868426]
13. Rosen EL, Blackwell KL, Baker JA, Soo MS, Bentley RC, Yu D, et al. Accuracy of MRI in the detection of residual breast cancer after neoadjuvant chemotherapy. AJR American journal of roentgenology. 2003; 181(5):1275–82.10.2214/ajr.181.5.1811275 [PubMed: 14573420]
14. Weatherall PT, Evans GF, Metzger GJ, Saborrian MH, Leitch AM. MRI vs. histologic measurement of breast cancer following chemotherapy: comparison with x-ray mammography and palpation. Journal of magnetic resonance imaging : JMRI. 2001; 13(6):868–75. [PubMed: 11382946]
15. Hylton NM, Blume JD, Bernreuter WK, Pisano ED, Rosen MA, Morris EA, et al. Locally advanced breast cancer: MR imaging for prediction of response to neoadjuvant chemotherapy--

results from ACRIN 6657/I-SPY TRIAL. Radiology. 2012; 263(3):663–72. Epub 2012/05/25. 10.1148/radiol.12110748 [PubMed: 22623692]

16. Lee CI, Bensink ME, Berry K, Musa Z, Bodnar C, Dann R, et al. Performance goals for an adjunct diagnostic test to reduce unnecessary biopsies after screening mammography: analysis of costs, benefits, and consequences. J Am Coll Radiol. 2013; 10(12):924–30.10.1016/j.jacr.2013.09.009 [PubMed: 24295942]
17. DeMartini W, Lehman C. A review of current evidence-based clinical applications for breast magnetic resonance imaging. Top Magn Reson Imaging. 2008; 19(3):143–50.10.1097/RMR.0b013e31818a40a5 [PubMed: 18941394]
18. Cilotti A, Iacconi C, Marini C, Moretti M, Mazzotta D, Traino C, et al. Contrast-enhanced MR imaging in patients with BI-RADS 3–5 microcalcifications. Radiol Med. 2007; 112(2):272–86.10.1007/s11547-007-0141-9 [PubMed: 17361370]
19. Bluemke DA, Gatsonis CA, Chen MH, DeAngelis GA, DeBruhl N, Harms S, et al. Magnetic resonance imaging of the breast prior to biopsy. JAMA. 2004; 292(22):2735–42.10.1001/jama.292.22.2735 [PubMed: 15585733]
20. Yau EJ, Gutierrez RL, DeMartini WB, Eby PR, Peacock S, Lehman CD. The utility of breast MRI as a problem-solving tool. Breast J. 2011; 17(3):273–80.10.1111/j.1524-4741.2011.01075.x [PubMed: 21477168]
21. Strobel K, Schrading S, Hansen NL, Barabasch A, Kuhl CK. Assessment of BI-RADS category 4 lesions detected with screening mammography and screening US: utility of MR imaging. Radiology. 2015; 274(2):343–51.10.1148/radiol.14140645 [PubMed: 25271857]
22. Wang LC, DeMartini WB, Partridge SC, Peacock S, Lehman CD. MRI-detected suspicious breast lesions: predictive values of kinetic features measured by computer-aided evaluation. AJR American journal of roentgenology. 2009; 193(3):826–31.10.2214/AJR.08.1335 [PubMed: 19696298]
23. Chen, H.; Olson, ML.; Partridge, SC.; Kerwin, W., editors. Reducing the scan time in quantitative dynamic contrast enhanced MRI of the breast using the extended graphical model; Proceedings of the ISMRM Annual Meeting; April 2013; Melbourne, Australia.
24. Pinker K, Bogner W, Baltzer P, Trattnig S, Gruber S, Abeyakoon O, et al. Clinical application of bilateral high temporal and spatial resolution dynamic contrast-enhanced magnetic resonance imaging of the breast at 7 T. European radiology. 2014; 24(4):913–20. Epub 2013/12/07. 10.1007/s00330-013-3075-8 [PubMed: 24306425]
25. Tudorica LA, Oh KY, Roy N, Kettler MD, Chen Y, Hemmingson SL, et al. A feasible high spatiotemporal resolution breast DCE-MRI protocol for clinical settings. Magnetic resonance imaging. 2012; 30(9):1257–67.10.1016/j.mri.2012.04.009 [PubMed: 22770687]
26. Kuhl CK, Mielcareck P, Klaschik S, Leutner C, Wardelmann E, Gieseke J, et al. Dynamic breast MR imaging: are signal intensity time course data useful for differential diagnosis of enhancing lesions? Radiology. 1999; 211(1):101–10.10.1148/radiology.211.1.r99ap38101 [PubMed: 10189459]
27. Tofts PS, Kermode AG. Measurement of the blood-brain barrier permeability and leakage space using dynamic MR imaging. 1. Fundamental concepts. Magnetic resonance in medicine. 1991; 17(2):357–67. [PubMed: 2062210]
28. Li L, Wang K, Sun X, Wang K, Sun Y, Zhang G, et al. Parameters of dynamic contrast-enhanced MRI as imaging markers for angiogenesis and proliferation in human breast cancer. Med Sci Monit. 2015; 21:376–82.10.12659/MSM.892534 [PubMed: 25640082]
29. Huang W, Tudorica LA, Li X, Thakur SB, Chen Y, Morris EA, et al. Discrimination of benign and malignant breast lesions by using shutter-speed dynamic contrast-enhanced MR imaging. Radiology. 2011; 261(2):394–403.10.1148/radiol.11102413 [PubMed: 21828189]
30. Marinovich ML, Sardanelli F, Ciatto S, Mamounas E, Brennan M, Macaskill P, et al. Early prediction of pathologic response to neoadjuvant therapy in breast cancer: systematic review of the accuracy of MRI. Breast. 2012; 21(5):669–77.10.1016/j.breast.2012.07.006 [PubMed: 22863284]
31. Kuhl CK, Kooijman H, Gieseke J, Schild HH. Effect of B1 inhomogeneity on breast MR imaging at 3.0 T. Radiology. 2007; 244(3):929–30. Epub 2007/08/22. 10.1148/radiol.2443070266 [PubMed: 17709843]

32. Tofts PS, Brix G, Buckley DL, Evelhoch JL, Henderson E, Knopp MV, et al. Estimating kinetic parameters from dynamic contrast-enhanced T(1)-weighted MRI of a diffusable tracer: standardized quantities and symbols. Journal of magnetic resonance imaging : JMRI. 1999; 10(3): 223–32. [PubMed: 10508281]
33. Yankeelov TE, Luci JJ, Lepage M, Li R, Debusk L, Lin PC, et al. Quantitative pharmacokinetic analysis of DCE-MRI data without an arterial input function: a reference region model. Magnetic resonance imaging. 2005; 23(4):519–29.10.1016/j.mri.2005.02.013 [PubMed: 15919597]
34. Huang W, Li X, Chen Y, Li X, Chang MC, Oborski MJ, et al. Variations of dynamic contrast-enhanced magnetic resonance imaging in evaluation of breast cancer therapy response: a multicenter data analysis challenge. Translational oncology. 2014; 7(1):153–66. [PubMed: 24772219]
35. Partridge SC, McDonald ES. Diffusion weighted magnetic resonance imaging of the breast: protocol optimization, interpretation, and clinical applications. Magn Reson Imaging Clin N Am. 2013; 21(3):601–24.10.1016/j.mric.2013.04.007 [PubMed: 23928248]
36. Guo Y, Cai YQ, Cai ZL, Gao YG, An NY, Ma L, et al. Differentiation of clinically benign and malignant breast lesions using diffusion-weighted imaging. Journal of magnetic resonance imaging : JMRI. 2002; 16(2):172–8. [PubMed: 12203765]
37. Le Bihan D, Breton E, Lallemand D, Grenier P, Cabanis E, Laval-Jeantet M. MR imaging of intravoxel incoherent motions: application to diffusion and perfusion in neurologic disorders. Radiology. 1986; 161(2):401–7.10.1148/radiology.161.2.3763909 [PubMed: 3763909]
38. Le Bihan D, Breton E, Lallemand D, Aubin ML, Vignaud J, Laval-Jeantet M. Separation of diffusion and perfusion in intravoxel incoherent motion MR imaging. Radiology. 1988; 168(2): 497–505.10.1148/radiology.168.2.3393671 [PubMed: 3393671]
39. Rubesova E, Grell AS, De Maertelaer V, Metens T, Chao SL, Lemort M. Quantitative diffusion imaging in breast cancer: a clinical prospective study. Journal of magnetic resonance imaging : JMRI. 2006; 24(2):319–24. [PubMed: 16786565]
40. Sinha S, Lucas-Quesada FA, Sinha U, DeBruhl N, Bassett LW. In vivo diffusion-weighted MRI of the breast: potential for lesion characterization. Journal of magnetic resonance imaging : JMRI. 2002; 15(6):693–704. [PubMed: 12112520]
41. Woodhams R, Matsunaga K, Kan S, Hata H, Ozaki M, Iwabuchi K, et al. ADC mapping of benign and malignant breast tumors. Magn Reson Med Sci. 2005; 4(1):35–42. [PubMed: 16127252]
42. Chen X, Li WL, Zhang YL, Wu Q, Guo YM, Bai ZL. Meta-analysis of quantitative diffusion-weighted MR imaging in the differential diagnosis of breast lesions. BMC cancer. 2010; 10:693.10.1186/1471-2407-10-693 [PubMed: 21189150]
43. Ei Khouli RH, Jacobs MA, Mezban SD, Huang P, Kamel IR, Macura KJ, et al. Diffusion-weighted imaging improves the diagnostic accuracy of conventional 3.0-T breast MR imaging. Radiology. 2010; 256(1):64–73.10.1148/radiol.10091367 [PubMed: 20574085]
44. Partridge SC, DeMartini WB, Kurland BF, Eby PR, White SW, Lehman CD. Quantitative diffusion-weighted imaging as an adjunct to conventional breast MRI for improved positive predictive value. AJR American journal of roentgenology. 2009; 193(6):1716–22.10.2214/AJR.08.2139 [PubMed: 19933670]
45. Pinker K, Baltzer P, Bogner W, Leithner D, Trattnig S, Zaric O, et al. Multiparametric MR Imaging with High-Resolution Dynamic Contrast-enhanced and Diffusion-weighted Imaging at 7 T Improves the Assessment of Breast Tumors: A Feasibility Study. Radiology. 2015; 276(2):360–70.10.1148/radiol.15141905 [PubMed: 25751227]
46. Rahbar H, Partridge SC, Demartini WB, Gutierrez RL, Allison KH, Peacock S, et al. In vivo assessment of ductal carcinoma in situ grade: a model incorporating dynamic contrast-enhanced and diffusion-weighted breast MR imaging parameters. Radiology. 2012; 263(2):374–82.10.1148/radiol.12111368 [PubMed: 22517955]
47. Pickles MD, Gibbs P, Lowry M, Turnbull LW. Diffusion changes precede size reduction in neoadjuvant treatment of breast cancer. Magnetic resonance imaging. 2006; 24(7):843–7.10.1016/j.mri.2005.11.005 [PubMed: 16916701]
48. Sharma U, Danishad KK, Seenu V, Jagannathan NR. Longitudinal study of the assessment by MRI and diffusion-weighted imaging of tumor response in patients with locally advanced breast cancer

undergoing neoadjuvant chemotherapy. NMR in biomedicine. 2009; 22(1):104–13.10.1002/nbm.1245 [PubMed: 18384182]

49. Richard R, Thomassin I, Chapellier M, Scemama A, de Cremoux P, Varna M, et al. Diffusion-weighted MRI in pretreatment prediction of response to neoadjuvant chemotherapy in patients with breast cancer. European radiology. 2013; 23(9):2420–31.10.1007/s00330-013-2850-x [PubMed: 23652844]
50. Partridge SC, Demartini WB, Kurland BF, Eby PR, White SW, Lehman CD. Differential diagnosis of mammographically and clinically occult breast lesions on diffusion-weighted MRI. Journal of magnetic resonance imaging : JMRI. 2010; 31(3):562–70.10.1002/jmri.22078 [PubMed: 20187198]
51. Yabuuchi H, Matsuo Y, Sunami S, Kamitani T, Kawanami S, Setoguchi T, et al. Detection of non-palpable breast cancer in asymptomatic women by using unenhanced diffusion-weighted and T2-weighted MR imaging: comparison with mammography and dynamic contrast-enhanced MR imaging. European radiology. 2011; 21(1):11–7.10.1007/s00330-010-1890-8 [PubMed: 20640898]
52. Partridge SC, Singer L, Sun R, Wilmes LJ, Klifa CS, Lehman CD, et al. Diffusion-weighted MRI: influence of intravoxel fat signal and breast density on breast tumor conspicuity and apparent diffusion coefficient measurements. Magnetic resonance imaging. 2011; 29(9):1215–21.10.1016/j.mri.2011.07.024 [PubMed: 21920686]
53. Bogner W, Pinker K, Zaric O, Baltzer P, Minarikova L, Porter D, et al. Bilateral diffusion-weighted MR imaging of breast tumors with submillimeter resolution using readout-segmented echo-planar imaging at 7 T. Radiology. 2015; 274(1):74–84.10.1148/radiol.14132340 [PubMed: 25341078]
54. Lee SK, Tan ET, Govenkar A, Hancu I. Dynamic slice-dependent shim and center frequency update in 3 T breast diffusion weighted imaging. Magnetic resonance in medicine. 2014; 71(5):1813–8.10.1002/mrm.24824 [PubMed: 23798360]
55. Singer L, Wilmes LJ, Saritas EU, Shankaranarayanan A, Proctor E, Wisner DJ, et al. High-resolution diffusion-weighted magnetic resonance imaging in patients with locally advanced breast cancer. Academic radiology. 2012; 19(5):526–34.10.1016/j.acra.2011.11.003 [PubMed: 22197382]
56. Teruel JR, Fjosne HE, Ostlie A, Holland D, Dale AM, Bathen TF, et al. Inhomogeneous static magnetic field-induced distortion correction applied to diffusion weighted MRI of the breast at 3T. Magnetic resonance in medicine. 201410.1002/mrm.25489
57. Bokacheva L, Kaplan JB, Giri DD, Patil S, Gnanasigamani M, Nyman CG, et al. Intravoxel incoherent motion diffusion-weighted MRI at 3.0 T differentiates malignant breast lesions from benign lesions and breast parenchyma. Journal of magnetic resonance imaging : JMRI. 2014; 40(4):813–23.10.1002/jmri.24462 [PubMed: 24273096]
58. Iima M, Yano K, Kataoka M, Umehana M, Murata K, Kanao S, et al. Quantitative Non-Gaussian Diffusion and Intravoxel Incoherent Motion Magnetic Resonance Imaging: Differentiation of Malignant and Benign Breast Lesions. Investigative radiology. 201410.1097/RLI.0000000000000094
59. Liu C, Liang C, Liu Z, Zhang S, Huang B. Intravoxel incoherent motion (IVIM) in evaluation of breast lesions: comparison with conventional DWI. European journal of radiology. 2013; 82(12):e782–9.10.1016/j.ejrad.2013.08.006 [PubMed: 24034833]
60. Sigmund EE, Cho GY, Kim S, Finn M, Moccaldi M, Jensen JH, et al. Intravoxel incoherent motion imaging of tumor microenvironment in locally advanced breast cancer. Magnetic resonance in medicine. 2011; 65(5):1437–47.10.1002/mrm.22740 [PubMed: 21287591]
61. Jensen JH, Helpern JA. MRI quantification of non-Gaussian water diffusion by kurtosis analysis. NMR in biomedicine. 2010; 23(7):698–710.10.1002/nbm.1518 [PubMed: 20632416]
62. Partridge SC, Ziadloo A, Murthy R, White SW, Peacock S, Eby PR, et al. Diffusion tensor MRI: preliminary anisotropy measures and mapping of breast tumors. Journal of magnetic resonance imaging : JMRI. 2010; 31(2):339–47.10.1002/jmri.22045 [PubMed: 20099346]
63. Baltzer PA, Schafer A, Dietzel M, Grassel D, Gajda M, Camara O, et al. Diffusion tensor magnetic resonance imaging of the breast: a pilot study. European radiology. 2011; 21(1):1–10.10.1007/s00330-010-1901-9 [PubMed: 20668860]

64. Eyal E, Shapiro-Feinberg M, Furman-Haran E, Grobgeld D, Golan T, Itzchak Y, et al. Parametric diffusion tensor imaging of the breast. Investigative radiology. 2012; 47(5):284–91.10.1097/RLI.0b013e3182438e5d [PubMed: 22472798]

65. Roebuck JR, Cecil KM, Schnall MD, Lenkinski RE. Human breast lesions: characterization with proton MR spectroscopy. Radiology. 1998; 209(1):269–75.10.1148/radiology.209.1.9769842 [PubMed: 9769842]

66. Gribbestad IS, Singstad TE, Nilsen G, Fjosne HE, Engan T, Haugen OA, et al. In vivo 1H MRS of normal breast and breast tumors using a dedicated double breast coil. Journal of magnetic resonance imaging : JMRI. 1998; 8(6):1191–7. [PubMed: 9848727]

67. Cecil KM, Schnall MD, Siegelman ES, Lenkinski RE. The evaluation of human breast lesions with magnetic resonance imaging and proton magnetic resonance spectroscopy. Breast Cancer Res Treat. 2001; 68(1):45–54. [PubMed: 11678308]

68. Yeung DK, Cheung HS, Tse GM. Human breast lesions: characterization with contrast-enhanced in vivo proton MR spectroscopy--initial results. Radiology. 2001; 220(1):40–6.10.1148/radiology.220.1.r01jl0240 [PubMed: 11425970]

69. Sitter B, Sonnewald U, Spraul M, Fjosne HE, Gribbestad IS. High-resolution magic angle spinning MRS of breast cancer tissue. NMR in biomedicine. 2002; 15(5):327–37.10.1002/nbm.775 [PubMed: 12203224]

70. Haddadin IS, McIntosh A, Meisamy S, Corum C, Styczynski Snyder AL, Powell NJ, et al. Metabolite quantification and high-field MRS in breast cancer. NMR in biomedicine. 2009; 22(1):65–76.10.1002/nbm.1217 [PubMed: 17957820]

71. Bolan PJ. Magnetic resonance spectroscopy of the breast: current status. Magn Reson Imaging Clin N Am. 2013; 21(3):625–39.10.1016/j.mric.2013.04.008 [PubMed: 23928249]

72. Bartella L, Morris EA, Dershaw DD, Liberman L, Thakur SB, Moskowitz C, et al. Proton MR spectroscopy with choline peak as malignancy marker improves positive predictive value for breast cancer diagnosis: preliminary study. Radiology. 2006; 239(3):686–92.10.1148/radiol.2393051046 [PubMed: 16603660]

73. Meisamy S, Bolan PJ, Baker EH, Pollema MG, Le CT, Kelcz F, et al. Adding in vivo quantitative 1H MR spectroscopy to improve diagnostic accuracy of breast MR imaging: preliminary results of observer performance study at 4.0 T. Radiology. 2005; 236(2):465–75.10.1148/radiol.2362040836 [PubMed: 16040903]

74. Bartella L, Thakur SB, Morris EA, Dershaw DD, Huang W, Chough E, et al. Enhancing nonmass lesions in the breast: evaluation with proton (1H) MR spectroscopy. Radiology. 2007; 245(1):80–7.10.1148/radiol.2451061639 [PubMed: 17885182]

75. Baltzer PA, Dietzel M. Breast lesions: diagnosis by using proton MR spectroscopy at 1.5 and 3.0 T--systematic review and meta-analysis. Radiology. 2013; 267(3):735–46.10.1148/radiol.13121856 [PubMed: 23468577]

76. Pinker K, Bogner W, Baltzer P, Gruber S, Bickel H, Brueck B, et al. Improved diagnostic accuracy with multiparametric magnetic resonance imaging of the breast using dynamic contrast-enhanced magnetic resonance imaging, diffusion-weighted imaging, and 3-dimensional proton magnetic resonance spectroscopic imaging. Investigative radiology. 2014; 49(6):421–30.10.1097/RLI.0000000000000029 [PubMed: 24566292]

77. Katz-Brull R, Lavin PT, Lenkinski RE. Clinical utility of proton magnetic resonance spectroscopy in characterizing breast lesions. J Natl Cancer Inst. 2002; 94(16):1197–203. [PubMed: 12189222]

78. Zhao C, Bolan PJ, Royce M, Lakkadi N, Eberhardt S, Sillerud L, et al. Quantitative mapping of total choline in healthy human breast using proton echo planar spectroscopic imaging (PEPSI) at 3 Tesla. Journal of magnetic resonance imaging : JMRI. 2012; 36(5):1113–23.10.1002/jmri.23748 [PubMed: 22782667]

79. Meisamy S, Bolan PJ, Baker EH, Bliss RL, Gulbahce E, Everson LI, et al. Neoadjuvant chemotherapy of locally advanced breast cancer: predicting response with in vivo (1)H MR spectroscopy--a pilot study at 4 T. Radiology. 2004; 233(2):424–31.10.1148/radiol.2332031285 [PubMed: 15516615]

80. Shin HJ, Baek HM, Cha JH, Kim HH. Evaluation of breast cancer using proton MR spectroscopy: total choline peak integral and signal-to-noise ratio as prognostic indicators. AJR American journal of roentgenology. 2012; 198(5):W488–97.10.2214/AJR.11.7292 [PubMed: 22528931]
81. Jacobs MA, Barker PB, Argani P, Ouwerkerk R, Bhujwalla ZM, Bluemke DA. Combined dynamic contrast enhanced breast MR and proton spectroscopic imaging: a feasibility study. Journal of magnetic resonance imaging : JMRI. 2005; 21(1):23–8.10.1002/jmri.20239 [PubMed: 15611934]
82. Danishad KK, Sharma U, Sah RG, Seenu V, Parshad R, Jagannathan NR. Assessment of therapeutic response of locally advanced breast cancer (LABC) patients undergoing neoadjuvant chemotherapy (NACT) monitored using sequential magnetic resonance spectroscopic imaging (MRSI). NMR in biomedicine. 2010; 23(3):233–41.10.1002/nbm.1436 [PubMed: 20175134]
83. Dorrius MD, Pijnappel RM, van der Weide Jansen MC, Jansen L, Kappert P, Oudkerk M, et al. The added value of quantitative multi-voxel MR spectroscopy in breast magnetic resonance imaging. European radiology. 2012; 22(4):915–22.10.1007/s00330-011-2322-0 [PubMed: 22076317]
84. Gruber S, Debski BK, Pinker K, Chmelik M, Grabner G, Helbich T, et al. Three-dimensional proton MR spectroscopic imaging at 3 T for the differentiation of benign and malignant breast lesions. Radiology. 2011; 261(3):752–61.10.1148/radiol.11102096 [PubMed: 21998046]
85. Hu J, Yu Y, Kou Z, Huang W, Jiang Q, Xuan Y, et al. A high spatial resolution 1H magnetic resonance spectroscopic imaging technique for breast cancer with a short echo time. Magnetic resonance imaging. 2008; 26(3):360–6.10.1016/j.mri.2007.07.004 [PubMed: 17904326]
86. Jacobs MA, Barker PB, Bottomley PA, Bhujwalla Z, Bluemke DA. Proton magnetic resonance spectroscopic imaging of human breast cancer: a preliminary study. Journal of magnetic resonance imaging : JMRI. 2004; 19(1):68–75.10.1002/jmri.10427 [PubMed: 14696222]
87. Klomp DW, van de Bank BL, Raaijmakers A, Korteweg MA, Possanzini C, Boer VO, et al. 31P MRSI and 1H MRS at 7 T: initial results in human breast cancer. NMR in biomedicine. 2011; 24(10):1337–42.10.1002/nbm.1696 [PubMed: 21433156]
88. Schmitz AM, Veldhuis WB, Menke-Pluijmers MB, van der Kemp WJ, van der Velden TA, Kock MC, et al. Multiparametric MRI With Dynamic Contrast Enhancement, Diffusion-Weighted Imaging, and 31-Phosphorus Spectroscopy at 7 T for Characterization of Breast Cancer. Investigative radiology. 201510.1097/RLI.0000000000000183
89. Sinkus R, Tanter M, Xydeas T, Catheline S, Bercoff J, Fink M. Viscoelastic shear properties of in vivo breast lesions measured by MR elastography. Magnetic resonance imaging. 2005; 23(2):159–65. Epub 2005/04/19. 10.1016/j.mri.2004.11.060 [PubMed: 15833607]
90. Klomp DW, Dula AN, Arlinghaus LR, Italiaander M, Dortch RD, Zu Z, et al. Amide proton transfer imaging of the human breast at 7T: development and reproducibility. NMR in biomedicine. 2013; 26(10):1271–7. Epub 2013/04/06. 10.1002/nbm.2947 [PubMed: 23559550]
91. Dula AN, Arlinghaus LR, Dortch RD, Dewey BE, Whisenant JG, Ayers GD, et al. Amide proton transfer imaging of the breast at 3 T: establishing reproducibility and possible feasibility assessing chemotherapy response. Magnetic resonance in medicine. 2013; 70(1):216–24. Epub 2012/08/22. 10.1002/mrm.24450 [PubMed: 22907893]
92. Medved M, Newstead GM, Fan X, Du YP, Olopade OI, Shimauchi A, et al. Fourier component imaging of water resonance in the human breast provides markers for malignancy. Phys Med Biol. 2009; 54(19):5767–79.10.1088/0031-9155/54/19/007 [PubMed: 19741276]
93. Ouwerkerk R, Jacobs MA, Macura KJ, Wolff AC, Stearns V, Mezban SD, et al. Elevated tissue sodium concentration in malignant breast lesions detected with non-invasive 23Na MRI. Breast Cancer Res Treat. 2007; 106(2):151–60.10.1007/s10549-006-9485-4 [PubMed: 17260093]
94. Jacobs MA, Ouwerkerk R, Wolff AC, Gabrielson E, Warzecha H, Jeter S, et al. Monitoring of neoadjuvant chemotherapy using multiparametric, (2)(3)Na sodium MR, and multimodality (PET/CT/MRI) imaging in locally advanced breast cancer. Breast Cancer Res Treat. 2011; 128(1): 119–26.10.1007/s10549-011-1442-1 [PubMed: 21455671]
95. Rakow-Penner R, Daniel B, Glover GH. Detecting blood oxygen level-dependent (BOLD) contrast in the breast. Journal of magnetic resonance imaging : JMRI. 2010; 32(1):120–9.10.1002/jmri.22227 [PubMed: 20578018]

96. Li SP, Taylor NJ, Makris A, Ah-See ML, Beresford MJ, Stirling JJ, et al. Primary human breast adenocarcinoma: imaging and histologic correlates of intrinsic susceptibility-weighted MR imaging before and during chemotherapy. Radiology. 2010; 257(3):643–52.10.1148/radiol.10100421 [PubMed: 20858850]

97. Tatum JL, Kelloff GJ, Gillies RJ, Arbeit JM, Brown JM, Chao KS, et al. Hypoxia: importance in tumor biology, noninvasive measurement by imaging, and value of its measurement in the management of cancer therapy. International journal of radiation biology. 2006; 82(10):699–757.10.1080/09553000601002324 [PubMed: 17118889]

98. Jiang L, Weatherall PT, McColl RW, Tripathy D, Mason RP. Blood oxygenation level-dependent (BOLD) contrast magnetic resonance imaging (MRI) for prediction of breast cancer chemotherapy response: a pilot study. Journal of magnetic resonance imaging : JMRI. 2013; 37(5):1083–92.10.1002/jmri.23891 [PubMed: 23124705]

99. Liu M, Guo X, Wang S, Jin M, Wang Y, Li J, et al. BOLD-MRI of breast invasive ductal carcinoma: correlation of R2* value and the expression of HIF-1alpha. European radiology. 2013; 23(12):3221–7.10.1007/s00330-013-2937-4 [PubMed: 23835924]

100. Jacobs MA, Stearns V, Wolff AC, Macura K, Argani P, Khouri N, et al. Multiparametric magnetic resonance imaging, spectroscopy and multinuclear ((2)(3)Na) imaging monitoring of preoperative chemotherapy for locally advanced breast cancer. Academic radiology. 2010; 17(12):1477–85.10.1016/j.acra.2010.07.009 [PubMed: 20863721]

101. Li X, Abramson RG, Arlinghaus LR, Kang H, Chakravarthy AB, Abramson VG, et al. Multiparametric magnetic resonance imaging for predicting pathological response after the first cycle of neoadjuvant chemotherapy in breast cancer. Investigative radiology. 2015; 50(4):195–204.10.1097/RLI.0000000000000100 [PubMed: 25360603]

102. American College of Radiology Imaging Network (ACRIN) 6657: Contrast-Enhanced Breast MRI (and 1H-MRS) for Evaluation of Patients Undergoing Neoadjuvant Treatment for Locally Advanced Breast Cancer. https://http://www.acrin.org/6657_protocol.aspx.

103. American College of Radiology Imaging Network (ACRIN) 6702: A Multi-Center Study Evaluating the Utility of Diffusion Weighted Imaging for Detection and Diagnosis of Breast Cancer. https://http://www.acrin.org/TabID/879/Default.aspx.

104. American College of Radiology Imaging Network (ACRIN) 6698: Diffusion Weighted MR Imaging Biomarkers for Assessment of Breast Cancer Response to Neoadjuvant Treatment: A sub-study of the I-SPY 2 TRIAL (Investigation of Serial Studies to Predict Your Therapeutic Response with Imaging And moLecular Analysis). https://http://www.acrin.org/TabID/825/Default.aspx.

Key Points

1. Current clinical breast MRI approaches focus on high morphologic detail and semi-quantitative kinetic information that allows high sensitivity and moderate specificity for breast cancer detection.
2. Advanced functional MRI parameters can improve the ability to assess biology in vivo using imaging correlates of vascularity, cellularity, and chemical composition of breast lesions.
3. Preliminary findings support the use of a functional, multiparametric breast approach to improve breast MRI specificity and the biological characterization of breast cancer.
4. Currently, technical challenges and a lack of standardization in approach limit applicability of many functional breast MRI techniques, which should be addressed with future research.

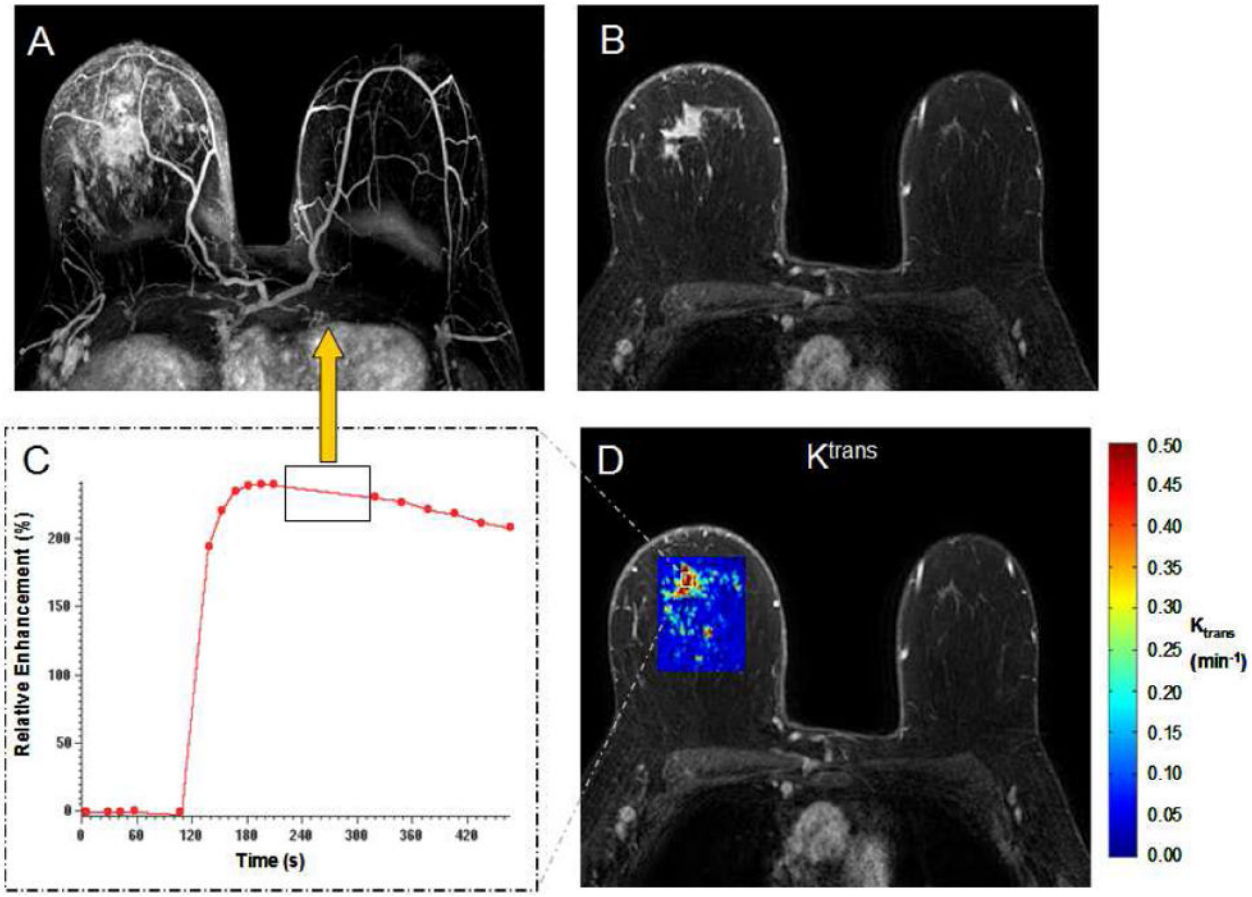

Fig. 1.

Novel combined high spatial and high temporal resolution DCE MRI scan approach, demonstrated in a subject with invasive ductal carcinoma. High spatial resolution phases (90 sec scan; 0.6×0.6×2mm resolution) are acquired before, 2 min, and 6.5 min post-contrast injection, interleaved with high temporal resolution dynamic 4D THRIVE (Philips Healthcare, Best, Netherlands) acquisitions (15 sec scan; 1×1×2 mm resolution). (A) Post-contrast subtraction maximum intensity projection generated from high spatial resolution images acquired at 2 min post-contrast injection. (B) Representative post-contrast high resolution image through the lesion. (C) Time-signal intensity curve showing contrast enhancement dynamics for region of interest in the invasive tumor. (D) Pharmacokinetic K^{trans} map calculated from the high temporal resolution images, overlaid on post-contrast image. Using this approach, three dimensional extent of disease, along with lesion morphology can be accurately assessed on post-contrast high spatial resolution images, while more rigorous pharmacokinetic modeling can be performed using corresponding high temporal resolution data acquired during the same scan. Adapted from Chen H, Olson ML, Partridge SC, Kerwin W, editors. Reducing the scan time in quantitative dynamic contrast enhanced MRI of the breast using the extended graphical model. Proceedings of the ISMRM Annual Meeting; April 2013; Melbourne, Australia.

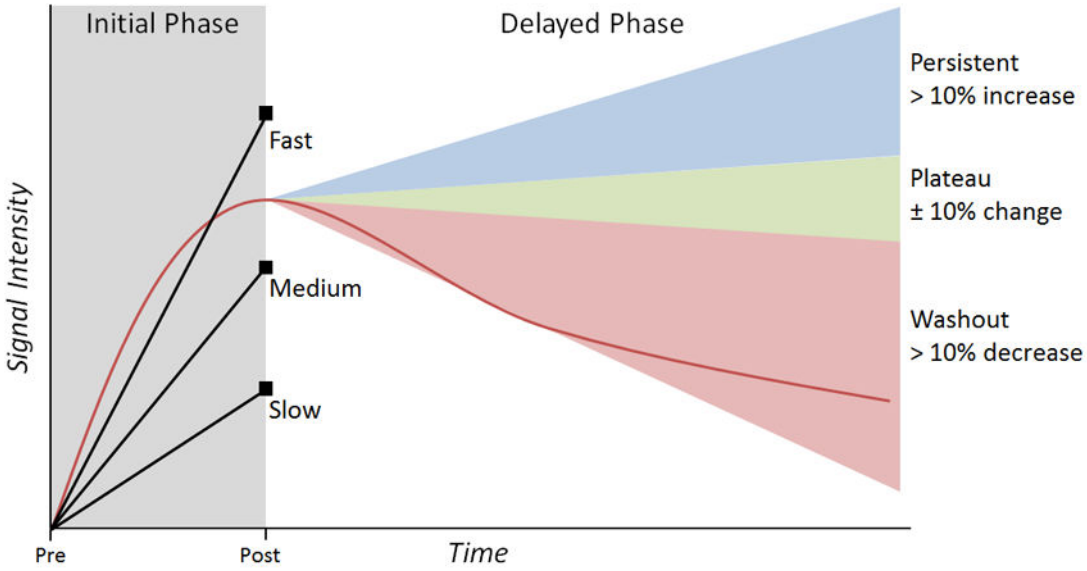

Fig. 2.

Semi-quantitative breast DCE kinetics analysis approach, as defined in the ACR BI-RADS atlas. The initial phase is classified based on the percent increase in signal intensity from pre-contrast levels, with increases of < 50%, 50–100%, and >100% classified as slow, medium, and fast, respectively. The delayed phase is classified by the curve type after initial peak enhancement as persistent (defined as a continuous increase in enhancement of greater than 10% initial enhancement), plateau (constant signal intensity once peak is reached ± 10% initial enhancement), or washout (decreasing signal intensity after peak enhancement greater than 10% initial enhancement).

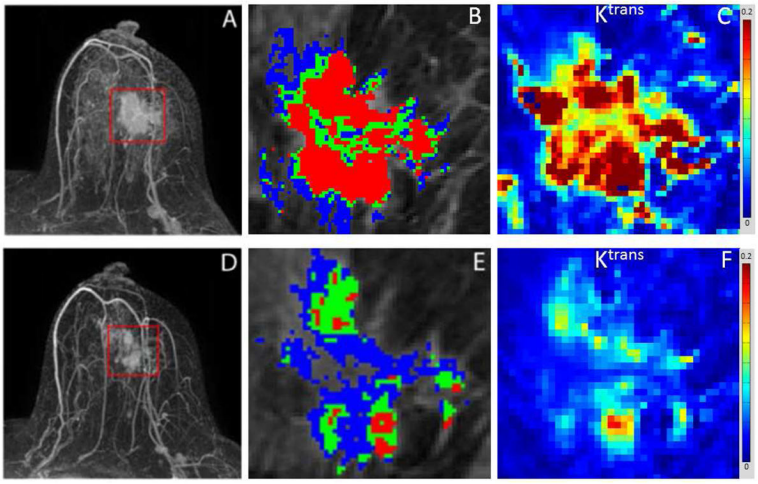

Fig. 3.

DCE-MRI in a 51-year-old woman undergoing neoadjuvant chemotherapy for invasive ductal carcinoma (Grade 3, ER+/PR+/HER2+). The subject was imaged prior to therapy (top; A–C) and 14 days after starting treatment with paclitaxel and trastuzumab (bottom; D–F). Shown are post-contrast subtraction maximum intensity projections (MIPs, left), color-coded curve type maps (blue = persistent enhancement, green = plateau enhancement, red = washout), and corresponding K^{trans} maps at each treatment time point. Changes in both lesion size and enhancement profile are evident at the early 2 week time point.

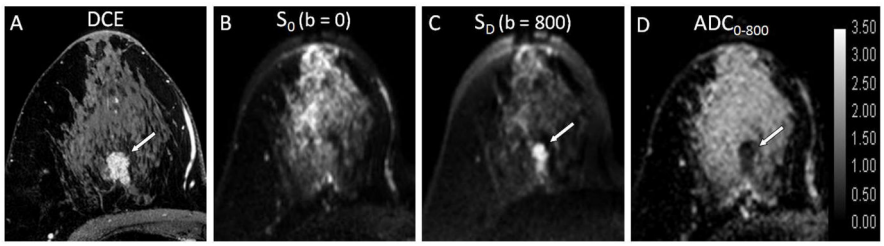

Fig. 4.

Example DWI images obtained in a 52-year-old woman with an invasive lobular breast cancer. (A) DCE-MRI post-contrast slice as reference. Shown are corresponding slices from DWI of (B) S_0 with b = 0 s/mm^2 (primarily T2-weighted), (C) S_D with b = 800 s/mm^2, and (D) apparent diffusion coefficient (ADC) map. The tumor (arrow) exhibits reduced diffusivity on DWI, appearing hyperintense on S_D (b = 800 s/mm^2) images (C) and hypointense (mean ADC = 0.89 ×10^{-3} mm^2/s) on the ADC map (D).

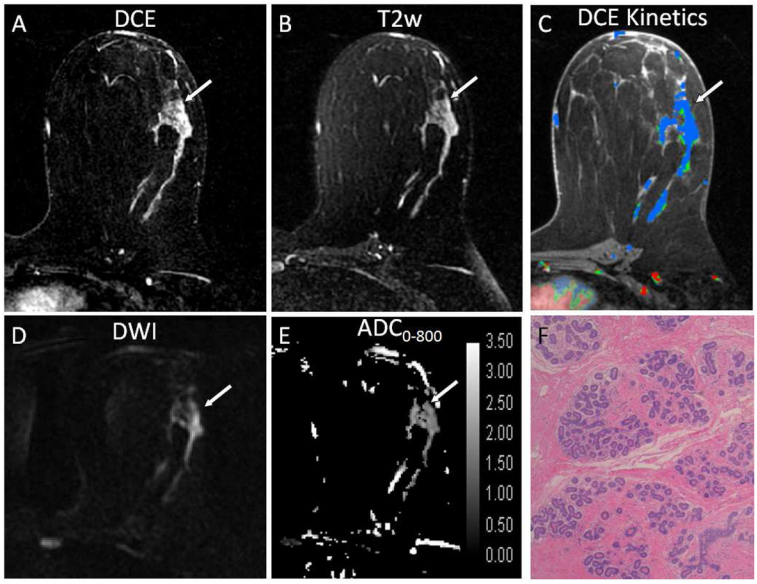

Fig. 5.

Benign adenosis breast lesion in a 34-year-old woman with a BRCA1 gene mutation who underwent 1.5T breast MRI high-risk screening. (A) Post-contrast T1-weighted subtraction image shows an 84 mm segmental area of nonmass enhancement in the left breast (arrows). (B) Axial T2-weighted image: The lesion is hyperintense. (C) DCE: The lesion shows mixed kinetics (96% delayed persistent enhancement [blue] and 4% delayed plateau enhancement [green]). (D) DWI ($b = 600$ s/mm^2): The lesion demonstrates hyperintensity. (E) ADC map: The lesion exhibits moderately high diffusivity, with a mean ADC of 1.68×10^{-3} mm^2/s. (F) Histologic examination (Hematoxylin-eosin stain; original magnification, ×40). (Adapted from Parsian S, Rahbar H, Allison KH, et al. Nonmalignant breast lesions: ADCs of benign and high-risk subtypes assessed as false-positive at dynamic enhanced MR imaging. Radiology 2012;265(3):696–706; with permission.)

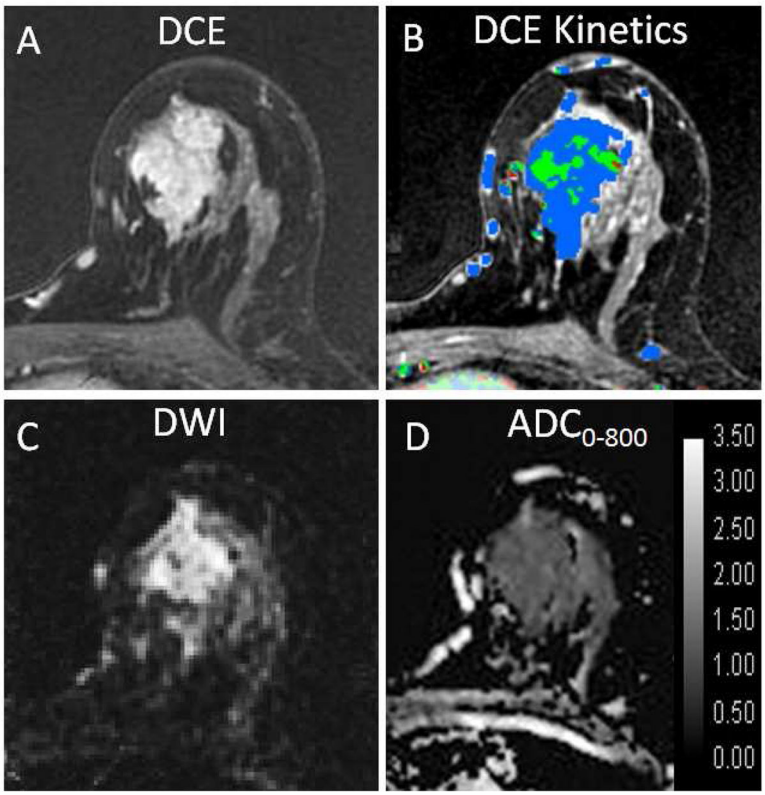

Fig. 6.

High grade ductal carcinoma in situ (DCIS) in 37-year-old woman who underwent 1.5T breast MRI. (A) Post-contrast T1-weighted fat-suppressed image shows a 51 mm enhancing lobular mass with irregular margins and heterogeneous internal and rapid enhancement in the left breast. (B) DCE-MRI: The mass demonstrates 146% peak initial enhancement with predominantly delayed persistent (blue) and plateau (green) enhancement kinetic features. (C) DWI (b = 600 sec/mm^2): The lesion demonstrates high signal intensity. (d) ADC map: The lesion demonstrates low diffusivity, with a mean ADC of 1.45×10^{-3} mm^2/s. (Adapted from Rahbar H, Partridge SC, DeMartini WB, et al. In vivo assessment of ductal carcinoma in situ grade: a model incorporating dynamic contrast-enhanced and diffusion-weighted breast MR imaging parameters. Radiology 2012;263(2):374–382; with permission.)

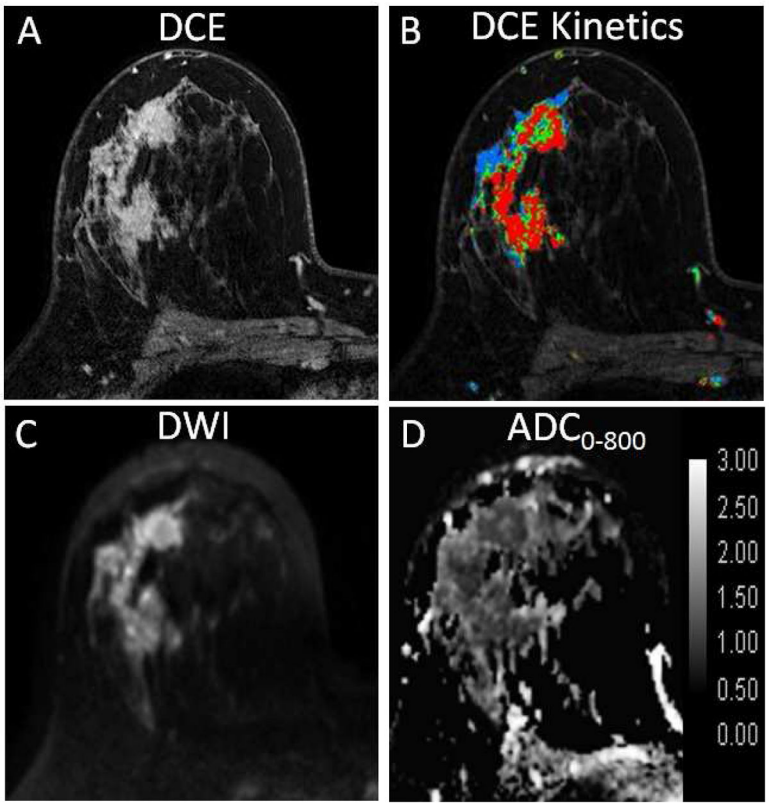

Fig. 7.

High grade invasive ductal carcinoma in a 35-year-old woman who underwent 3T breast MRI. (A) Post-contrast T1-weighted fat-suppressed image shows a large 47 mm enhancing irregular mass with heterogeneous internal and rapid enhancement in the right breast. (B) DCE-MRI: The mass demonstrates 489% peak initial enhancement with 66% delayed washout (red). (C) DWI ($b = 800$ s/mm^2): The lesion demonstrates high signal intensity. (D) ADC map: The lesion demonstrates low diffusivity, with a mean ADC of 0.94×10^{-3} mm^2/s.

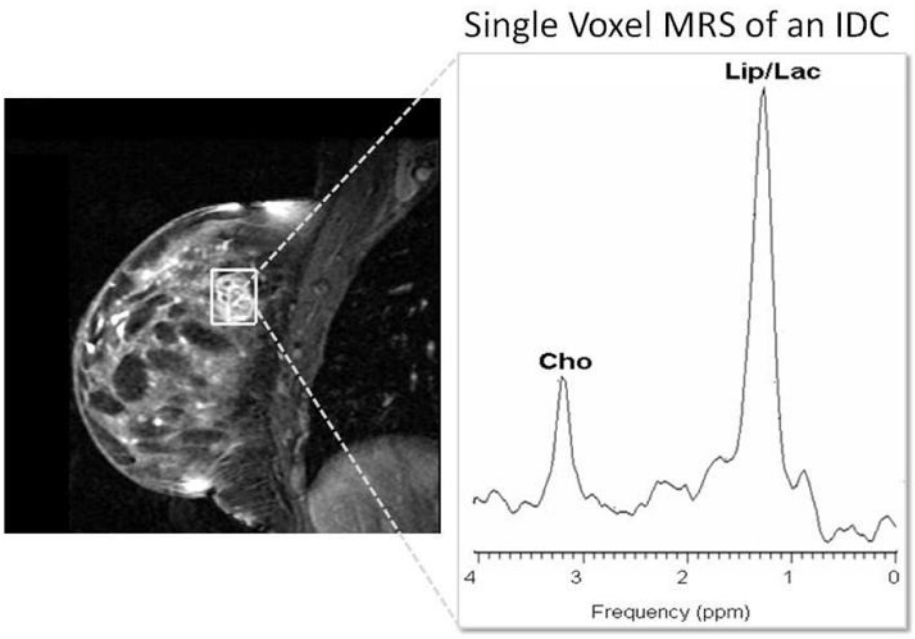

Fig. 8.

Example of single voxel breast ^{1}H MR spectra acquired at 1.5T in a patient with invasive ductal carcinoma (2.1 cm, grade 2). (A) The voxel was positioned encompassing the enhancing lesion as indicated on the sagittal postcontrast T1-weighted image. (B) The resulting spectra demonstrated a choline (tCho) peak at 3.2 ppm. Courtesy of Wei Huang, PhD, Oregon Health & Science University.